
Time-Varying Correlation Networks for Interpretable Change Point Detection

Kopal Garg
University of Toronto

Sana Tonekaboni
University of Toronto

Anna Goldenberg
University of Toronto

Abstract

Change point detection (CPD) methods aim to detect abrupt changes in time-series data. Recent CPD methods have demonstrated their potential in identifying changes in underlying statistical distributions but often fail to capture complex changes in the correlation structure in time-series data. These methods also fail to generalize effectively, as even within the same time-series, different kinds of change points (CPs) may arise that are best characterized by different types of time-series perturbations. To address this issue, we propose TiVaCPD, a CPD methodology that uses a time-varying graphical lasso based method to identify changes in correlation patterns between features over time, and combines that with an aggregate Kernel Maximum Mean Discrepancy (MMD) test to identify subtle changes in the underlying statistical distributions of dynamically established time windows. We evaluate the performance of TiVaCPD in identifying and characterizing various types of CPs in time-series and show that our method outperforms current state-of-the-art CPD methods for all categories of CPs.

1 Introduction

Change point detection (CPD) methods decompose time-series into disjoint segments with similar underlying properties. Accurately inferring time-points associated with such transitions is essential in deciphering the behaviors of the processes being modeled [Aminikhanghahi and Cook, 2017]. With a substantial increase in the volume of time-series data gathered in a variety of domains such as finance [Lavielle and Teyssi re, 2007] and healthcare [Yang et al., 2007], the importance of methods that automatically capture changes in the signal has grown. For instance, time-series collected from wearable devices and activity logs

describe a sequences of events like walking, standing or running. CPD methods allow us to identify and locate the transition between these states, without any labeled information about the states.

Most existing CPD methods fail to consider the underlying variability in the properties of change points (CPs) and therefore can not generalize effectively to complex time-series. CPs in time-series can be characterized as changes in the distribution of the measurements over time. Alternatively, these also could be changes in the correlation structure between time-series features. The former is more studied in the literature, however the later is also of significance in many applications. For instance, among physiological signals, the Heart Rate Variability (HRV) measure is always negatively correlated with Heart Rate (HR) measurement, but under some rare situations, they might exhibit a positive correlation, which indicates a potentially concerning change in the underlying state of an individual. Methods that solely rely on statistical distributions will fail to identify changes in time-varying dependencies in these scenarios.

In this paper, we propose a statistical CPD scoring method that captures different types of CPs in time-series without the need for labeled instances of change. More precisely, our CP score can be broken down into two parts identifying: 1) change in the covariance of the joint distribution of features over time, 2) change in the underlying distribution of the time-series feature measurements. Each part of the score is interpretable, allowing us to characterize and classify the CPs with similar underlying properties. To identify changes in the distributions, we build upon recent statistical results by Schrab et al. [2021] in the theory of non-parametric two-sample MMD tests aggregated with different kernel bandwidths. By dynamically adjusting the sliding window size, we address these concerns around model performance sensitivity. To identify the changes in the joint distribution of features over time, we rely on the hypothesis that changes in feature interactions can be effectively captured via correlation networks reconstructed from adjacent windows of time. To this end, we employ a dynamic network inference method, time-varying graphical lasso (TVGL) [Hallac et al., 2017], to acquire sparse time-varying precision matrices for detecting changes in

feature correlation patterns. We tested our method’s ability in identifying various categories of CPs on 4 simulated and 2 real-life time series datasets and compared its performance against 3 state-of-the-art CPD methods. The results show that our method outperforms all baselines on different datasets. The main contributions of this work are five-fold:

- We propose a statistical CPD method to detect and characterize different types of CPs in distribution shift or specific changes in feature dynamics.
- We propose a method to overcome the limitations of using static windows in existing approaches for distribution shift detection.
- We present a novel use of Time-Varying Graphical Lasso for quantifying changes in feature interactions. We demonstrate its capability in detecting CPs that occur due to changes in the covariance of the joint distribution of features over time.
- We introduce a post-processing procedure for ensembling the two parts of TiVaCPD scores. This involves using the Savitsky-Golay filter [Press and Teukolsky, 1990] to find smoothed estimates of individual scores while preserving local minima and maxima, and a multi-scale peak detection method for identifying local peaks and effectively reducing false positives.
- We demonstrate the interpretable nature of our method by identifying and classifying CPs into categories that pinpoint to variations in either statistical distribution or feature interactions.

2 Related Work

There are numerous supervised and unsupervised methods introduced for CPD in the literature, and a number of surveys that compare and contrast these methods for different applications [Truong et al., 2018, Aminikhanghahi and Cook, 2017, Reeves et al., 2007]. In this section, we will touch upon a few most relevant methods. The majority of methods formulate the problem in a way that assumes a time-series to be a collection of random variables with abrupt changes in distributional properties over time. Deciding between parametric and non-parametric techniques is dependent on the prior knowledge one wants to encode into the problem. Parametric methods [Gustafsson, 1996, Kawahara et al., 2007] that represent time intervals using Probability Density Functions [Yamanishi and Takeuchi, 2002] or auto-regressive models [Basseville and Nikiforov, 1993] can detect limited types of CPs. Non-parametric methods [Chang et al., 2019, Cheng et al., 2020, Matteson and James, 2014] are used in cases where the time-series dynamics cannot be easily modeled, and prior assumptions about the data distribution cannot be made. An optimal

transport-based method proposed by Cheng et al. [2020], conducts Wasserstein two-sample tests between the cumulative distribution functions of contiguous subsequences. Like other non-parametric methods it employs sliding windows of a fixed size to compute the test statistic. However, basing CP decisions on the local maxima of this statistic can be insufficient to control false positives. Another drawback of this method is that it projects the data onto several one-dimensional directions and uses the mean statistic, which can lead to the loss of detection power.

By using kernel functions, many CPD methods [Li et al., 2015] offer greater flexibility in representing the density functions of intervals of time. A deep learning based non-parametric method, KLCPD, Chang et al. [2019], uses deep generative models to increase test power of the kernel two-sample MMD test statistic [Gretton et al., 2007]. It addresses a few shortcomings of prior kernel-based CPD methods by efficiently eliminating the need to specify a fixed number of CPs, or relying on prior knowledge of a reference or training set for calibrating a kernel. However, as is the case with most single kernel-based MMD tests, its performance depends on the choice of kernel and kernel bandwidths.

Different categories of CPD methods may detect different statistical changes. Methods like KLCPD identify if changes in some moment of the distribution have occurred, as opposed to focusing on detecting a specific statistical parameter like the mean or variance. Even so, current methods often fail to capture changes in correlation patterns that occur due to evolving dynamics of multi-variate time-series. To address such CPs, Gibberd and Nelson [2015] introduced GraphTime; A Group-Fused Graphical Lasso estimator for grouped estimation of CPs in dependency structures of a time-series captured by a dynamic Gaussian Graphical Model. As the estimated graph topology is piece-wise constant, this is useful only when we’re interested in detecting jump points and abrupt changes, and leads to lots of false positives for other gradual CPs.

3 Method

3.1 Problem Formulation

Consider a multivariate time-series sample $\mathbf{X} \in \mathbb{R}^{d \times T}$ to be a sequence of random variables $[X_1, X_2, \dots, X_T]$ with d indicating the number of features in \mathbf{X} and T the total number of steps over time. Our goal is to identify the time steps that are CPs in the data sample \mathbf{X} . This is done by estimating a score $S[t], \forall t \in [T]$ that measures the amount of change in the generative distribution of the time points.

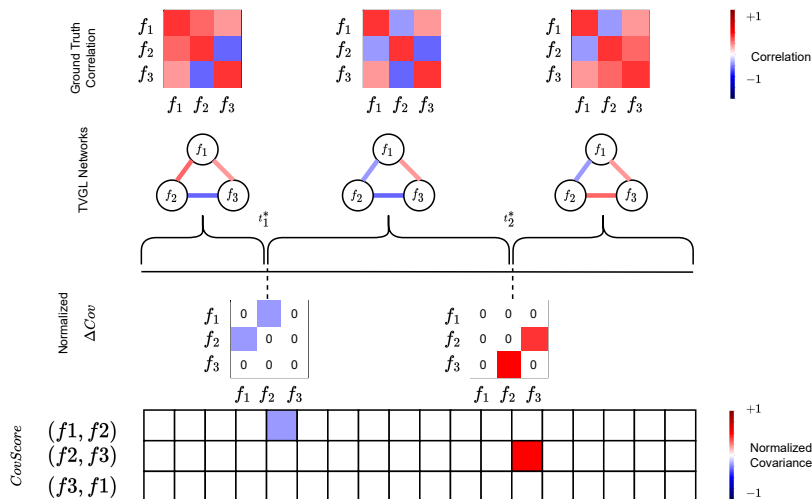


Figure 1: Estimating the change in feature dynamics over time using Time Varying Graphical Lasso (TVGL). This example shows the dynamics of 3 features of a sample over time. Changes in interactions between features in consecutive time windows are represented through correlation matrices. The resulting scores are presented in form of a heatmap, each row showing the changes in correlation among a pair of features f . The sign of ΔCov represents the direction of change, and the score value represents the magnitude of change.

3.2 Our CPD Algorithm-TiVaCPD

In this section, we introduce our CPD algorithm called Time Variable Change Point Detection TiVaCPD. The score S generated by TiVaCPD is composed of two main components, each measuring a different type of change in the distribution of the data. In the following section, we introduce each component separately, explain how they result in a unifying score that captures a variety of CP types, and describe how to interpret the score to better understand the CP.

3.2.1 Detecting changes in correlation structure using Time-Varying Graphical Lasso

In multivariate time-series the dynamics of features may evolve over time, and this can be modeled using graphical approaches. Precisely, at every time point, the feature interactions can be modelled as a graph network, with nodes corresponding to each feature, and the links corresponding to correlation between sets of variables (Figure 1). An abrupt change in the network indicates a change in the joint distribution of the features and is considered a CP in the time-series signal. We use the Time-Varying Graphical Lasso (TVGL) [Hallac et al., 2017] to infer the structure of the graph networks by estimating a sparse time-varying inverse covariance matrix Σ_t^{-1} of size $[d \times d]$ for all $t \in [T]$ in the time series observations. The inverse covariance matrix, or the weighted adjacency matrix of the graph, encodes the dependence between pairs of variables. $\Sigma_{i,j}^{-1} = 0$ implies conditional independence, and $\Sigma_{i,j}^{-1} \neq 0$ implies a structural dependency between i and j at a given

time. Using a lasso penalty, TVGL enforces sparsity in the covariance matrix by penalizing the weights of edges between variables and selecting only a few connections by forcing most edges to 0, thus providing interpretable results [Hallac et al., 2017]. With increasing number of features and longer time-series samples, dynamic network inference can become computationally expensive. TVGL uses a scalable message-passing algorithm called Alternating Direction Method of Multipliers to estimate the inverse sparse covariance matrices efficiently.

Learning these covariance estimates from windows of data reveals the underlying evolutionary patterns present in the time-series. We employ this technique to identify points of changes in feature interactions between adjacent local windows of time. By taking the difference between the absolute values of adjacent precision matrices, we quantify these changes in the distribution. A value close to 0 in this matrix indicates nearly identical estimations of the network, and hence no CP in that feature interaction (see Algorithm 1). A negative value indicates a positive correlation change, and a positive value indicates a negative correlation change. We set the diagonals of the normalized matrix of differences to 0, and set the score for a given time point to the sum of the elements in the lower triangle. As the dynamics of features evolves over time, a significant change in covariance for any of the feature pairs can indicate a CP. Investigating the pair-wise changes enables us to explain and understand the CPs.

There are two regularization parameters used in TVGL - α and β , where α is a measure of network sparsity, while β

Algorithm 1 TVCov

-
- 1: **Input:** \mathbf{X} (multivariate time series), α (regularization parameter controlling the network sparsity), β (parameter controlling the temporal consistency), $SliceSize$ (number of samples in each slice, or timestamp)
 - 2: **Output:** $CovScore$ (score representing change in adjacent precision matrices)
 - 3: $P = TVGL(\mathbf{X}, \alpha, \beta, SliceSize)$ // Sparse inverse covariance $\forall t \in [1, \dots, T]$
 - 4: **for all** $t \in [1, \dots, T]$ **do**
 - 5: $CovScore[t] = \begin{cases} \sum(|P[t]| - |P[t-1]|) & \text{if } t > 0 \\ 0 & \text{if } t = 0 \end{cases}$
 - 6: **return** $CovScore$
-

controls temporal consistency by determining how strongly correlated adjacent network estimations should be. Small α values lead to very dense networks that are less interpretable as the model overfits the data. Large β values lead to smoother network estimates over time that don't easily change from window to window. Another parameter, slice size, represents the number of samples present in each timestamp. The performance of our method slightly varies depending on parameter settings, but in general, choosing a high alpha value, a small beta value and a small slice size leads to more granular, timely and interpretable CPs.

3.2.2 Detecting shift in distribution using dynamic MMD Aggregate

Assuming in a time-series sample \mathbf{X} , each X_t is independently generated from a joint probability distribution $P_t(\cdot)$, a CP occurs at time t^* if observations after t^* are generated from an underlying distribution with a statistically significant difference from the distribution generating values prior to t^* . To compare the probability distributions of adjacent windows, we employ a non-parametric two-sample testing procedure called MMD Aggregate (MMDAgg), introduced in Schrab et al. [2021]. Let Δ^- be the number of observations of X before a query point t , and let this prior window be denoted by $X_{\Delta^-}^t = X_{t-\Delta^-}, \dots, X_{t-1}, X_t$. Similarly, the window of future observations can be denoted by $X_{\Delta^+}^t = X_{t+1}, \dots, X_{t+\Delta^+-1}, X_{t+\Delta^+}$, where Δ^+ represents the future window length. Kernel-based Maximum Mean Discrepancy (MMD) tests serve as a measure between two probability distributions. With the statistical test threshold α , if the null hypothesis, $H_0 : p < \alpha$, is rejected, the time-series may be partitioned by a CP t^* , signifying that measurements in the $X_{t^*-\Delta^-:t^*}$ windows come from a different distribution than measurements in $X_{t^*+1:\Delta^+}$. The performance of a single kernel-based MMD test typically depends on the choice of kernel and kernel bandwidths. A common approach for selecting kernel bandwidths used by the state-of-the-art MMD tests involves setting the bandwidths equal to the median inter-sample distance [Schrab et al., 2021]. Another approach involves di-

viding the data into two parts, and using the first half for bandwidth selection and the second half for conducting the test [Gretton et al., 2012]. Although better than the median heuristic approach which has no theoretical guarantees, this approach suffers from a loss of power caused by using only half of the data for running the test [Schrab et al., 2021]. Since we compare adjacent windows with restricted number of samples, any loss of data to kernel bandwidth selection can be detrimental to our method's performance. To overcome this problem, MMDAgg aggregates multiple MMD tests using different kernel bandwidths, ensuring maximized test power over the collection of kernels used, and eliminating the need for data splitting or arbitrary kernel selection. The method considers a finite collection Λ of d bandwidths, where the aggregated test is defined as a test which rejects H_0 if one of the tests over given bandwidth rejects H_0 .

Another challenge with Kernel-based MMD methods is choosing the right window size. Existing CPD methods that use statistical testing for determining a shift in the data distribution employ a sliding window approach with fixed-length that shift by unit increments to create instances. A key problem with this assumption is that it introduces the need to fine-tune the window size, as the overall performance of the method relies heavily on the choice of window size. Large window sizes may cause the method to overlook smaller CPs, while smaller window sizes may contribute to accumulation of error and hinder the power of the statistical test by limiting the number of samples. To address this challenge, we propose to dynamically establish the window size based on the presence of CPs (Algorithm 2). Let Δ^- represent the size of the dynamic window of data points from the last estimated CP, \hat{t} , up until the current time point, t . Starting with a constant Δ^+ and a small Δ^- window, the running window length is dynamically established by increasing Δ^- until a new CP is occurred, which is indicated by the aggregate MMD test. If a significant change in distribution isn't detected by the MMD test, i.e. the MMD score is smaller than a pre-defined threshold ϵ , the two sub-sequences are combined and compared against the next sub-sequence in the series. This way we generate a new Δ^- window only when a CP is detected. This process is also explained in Figure 2. Our approach eliminates the need for doing repetitive comparisons between fixed-size symmetric windows and takes advantage of a growing set of samples for the MMD test. The MMD scores generated using the dynamic windowing indicate the CPs in time when the generative distribution of the data shifts.

For determining the final CP score, we need to meaningfully ensemble the MMD score with the CovScore, and this can be challenging because the covariance score is bounded while MMD is a positive unbounded score. Hence, we incorporated kernel normalization in the MMDAgg algorithm. Typically, to normalize a kernel so as to have a sim-

Algorithm 2 Dynamic MMD

```

1: Input: Time series  $\mathbf{X}$ ,  $\alpha$  (Statistical test threshold),
    $\Delta^-$  (Initial previous window size),  $\Delta^+$  (Future window size),  $\epsilon$  (Threshold for significance)
2: Output: DistScore
3:  $\delta = \Delta^-$  // Size of the running window
4: for all  $t \in [1, \dots, T]$  do
5:    $prev = X[t - \delta : t, :]$ 
6:    $next = X[t : t + \Delta^+, :]$ 
7:   if  $score \geq \epsilon$  then
8:      $\delta = \Delta^-$ 
9:      $DistScore[t] = \text{MMDAgg}(\mathbf{X}, prev, next, \alpha)$ 
10:  else
11:     $\delta = \delta + 1$ 
12:     $DistScore[t] = 0$ 
13: return  $DistScore$ 
    
```

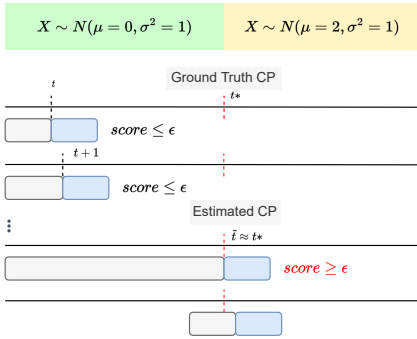


Figure 2: Dynamic windowing procedure for measuring the DistScore. The gray box shows the previous windows size, and the blue box shows the window for future observation. As we proceed over time and as long as we don’t encounter a CP, \tilde{t} , the size of the previous window grows to include more samples from the generative distribution. Once a CP is detected (third row), the size of the window reduces to the initial window size.

ilarity index, cosine normalization is applied. Instead, we use a generalization of the cosine normalization [Ah-Pine, 2010]. For a given kernel function, $K^{z=1}(x, y)$ represents the normalized kernel of order z . We use the generalized mean with exponent $z = 1$ (arithmetic mean), which for a set of p values $a_{i=1}^p = a_1, a_2, \dots, a_p$ is defined as follows:

$$M^{z=1}(a_{i=1}^p) = \frac{1}{p} \sum_{i=1}^p (a_i^z) \quad (1)$$

Where $K^{z=1}(x, y) = \frac{K(x, y)}{M^{z=1}(K(x, x), K(y, y))}$. This normalization technique projects the objects from the feature space to a unit hypersphere, and guarantees $|K^{z=1}(x, y)| \leq 1$. As the final step, we apply the same low-order digital smoothing polynomial filter to the raw DistScore.

3.3 Ensemble Score and CP Classification

As the final step, we combine the scores obtained using Algorithm 1 and Algorithm 2 to generate a unified score, as shown in Algorithm 3. We apply Savitzky Golay, a low-order digital smoothing polynomial filter, to individual score components and add both filtered components [Press and Teukolsky, 1990] to form a unified metric. Filtering the scores individually reduces the number of spurious CPs, and coalesces nearby peaks that represent the same CP while avoiding time-local smearing of the signal of interest. We use an adaptive scale selection-based peak detection approach [Scholkman et al., 2012] to locate the exact times for the CPs. The algorithm compares neighboring scores and finds the local maxima that includes minor peaks that are isolated relative to other major peaks, but may still represent plausible CPs in their own local region.

3.4 Understanding and interpreting TiVaCPD score

One of the advantages of our method is that in addition to identifying CPs, it can also provide an understanding of the underlying characteristic of the change. In real-world cases, a mixture of CPs can occur. The DistScore can be used to identify changes in the underlying distribution of the time-series’ feature measurements. The CovScore can be used to understand the specific changes in feature dynamics, specifically a change of the correlation structure of two features. At each time step, the CovScore represents the pair-wise interaction between variables, i.e. the normalized difference between neighboring precision matrices. With this information, we are able to classify CPs into different categories, improving interpretability.

Figure 3, aims to illustrate this point. CPs 1 and 2 occur only due to a change in correlation between features 0 and 1, CP 3 occurs due to a change in correlation between features 0 and 1, as well as a change in mean and variance, CP 4 occurs due to a change in correlation, and a change in mean. Through this approach, we can identify not just one pair, but multiple pairs of features that may change with respect to each other at a given point in time as well as the direction in which the change happens. TiVaCPD correctly identifies that CPs 1 and 3 occur due to negative changes in correlation, whereas CPs 2 and 4 occur due to positive changes in correlation. This provides another means of further sub-categorizing such CPs. For example in the Heart Rate Variability (HRV) example, if HRV and HR change from being inversely correlated to being positively correlated, it may be indicative of an adverse health event. In such cases, knowing more than just when a CP happens, and understanding the underlying modification in feature dynamics can be useful for interpreting the CPs. The heatmap from the CovScore tells us the exact pair of features that resulted in a CP.

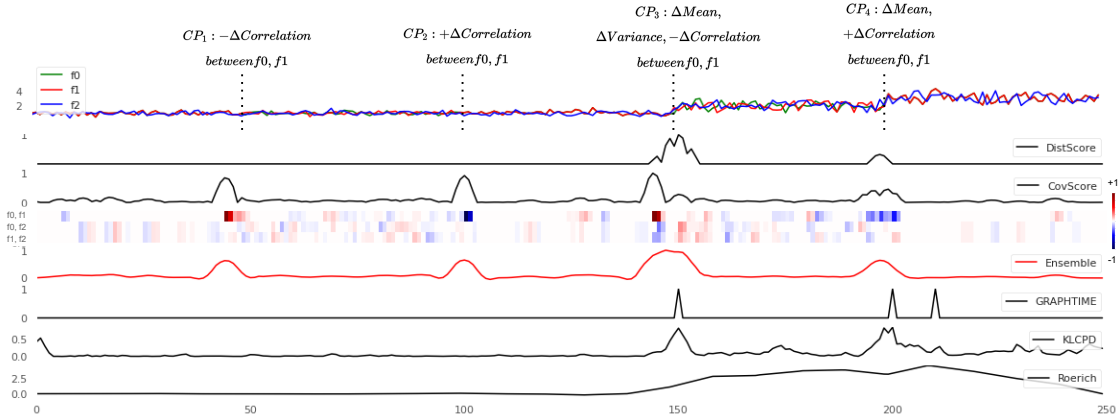


Figure 3: An example of a simulated time series with various kinds of CPs (caused by change in correlation and mean or variance). The first row from the top represents the raw signal. Rows Rows 2-5 represent the decomposition of the TiVaCPD score, and rows 6-8 represent CP estimation scores of other baselines.

Algorithm 3 TiVaCPD

- 1: **Input:** \mathbf{X} , α (Parameter controlling the network sparsity), β (Parameter controlling the temporal consistency), $SliceSize$ (Number of samples in each slice, or timestamp), α_1 (Statistical test threshold), ϵ (CPD acceptance threshold), Δ^- (Initial previous window size), Δ^+ (Future window size)
 - 2: **Output:** **TiVaCPD score**
 - 3: $CovScore = TVCov(\mathbf{X}, \alpha, \beta, SliceSize)$
 - 4: $DistScore = DynamicMMD(\mathbf{X}, \Delta^-, \Delta^+, \alpha_1, \epsilon)$
 - 5: **for all** $t \in [T]$ **do**
 - 6: $S[t] = |Savitzky-Golay(CovScore[t])| + |Savitzky-Golay(DistScore[t])|$
 - 7: $CP = AdaptivePeakFinding(S)$
 - 8: **return** CP, S
-

4 Experiments

4.1 Datasets

We demonstrate the performance of our method in comparison to multiple baselines on four simulated and two real-life multivariate data sets commonly used in the CPD literature. Different simulations test the functionality of CPD methods on a variety of potential CP scenarios.

4.1.1 Simulated data

In all our simulated datasets, each time series sample $\mathbf{X} \in \mathbb{R}^{d \times T}$ consists of $d = 3$ features. Each measurement $x_{i,t}$ for $i \in [d]$ and $t \in [T]$ is sampled independently from a Gaussian distribution $x_{i,t} \sim N(\mu_{i,t}, \sigma_{i,t}^2)$. We introduce different CPs as described below:

Jumping Mean For this data set, the variance is assumed to be constant over time and across all features and is set to $\sigma^2 = 0.5$. The ground truth CPs correspond to abrupt jumps in the mean that can happen independently in any of the features.

Changing Variance In this dataset, all three features are generated with constant mean $\mu = 1$ but their distribution variance changes over time. The CPs are indicated as time points with changes in σ^2 .

Changing Correlation This data set consists of a multivariate time-series generated with constant σ^2 and μ . To introduce correlation changes between variables, feature 2 is modified to be: $\widetilde{x}_{2,t} = \rho_t \times x_{1,t} + \sqrt{(1 - \rho_t^2)} \times x_{2,t}$, where ρ_t controls the correlation between the 2 features that can vary over time and is randomly sampled from $[-1, 1]$. Here the ground truth CPs correspond to points in time where the correlation ρ_t changes.

Arbitrary CPs This data set consists of a multivariate time-series with CPs due to varying μ , or σ^2 , or correlations between pairs of variables, resulting in a mixture of CPs scattered over time.

4.1.2 Bee dance

The Bee Dance dataset [Min Oh et al., 2008] consists of six three dimensional time-series of bees' positions while performing three-stage waggle dances. The bees communicate through actions like left turn, right turn and waggle, and the transition between these states represent ground truth CP.

4.1.3 Human Activity Recognition (HAR)

We use a subset of the HAR [Anguita et al., 2013] that provides periods of human activity. The six activities carried out by the subjects are normal walking, walking upstairs, walking downstairs, standing, sitting, and laying. These are measured with 3-axial linear acceleration and 3-axial angular velocity sensors, for a total of 6 features. The ground truth CPs are labeled as the transitions between activities.

4.2 Baseline Methods and Hyperparameter Settings

We compare the performance of TiVaCPD with a number of state-of-the-art CPD methods as explained below.¹ We have selected methods from different categories of CPD, namely methods that measure change in distribution, and methods that rely mostly on the graphical structure of the features over time. This way we can assess how different approaches perform for various types of CPs.

Kernel Change Point Detection (KLCPD) [Chang et al., 2019] KLCPD is a kernel learning framework for CPD that uses a two-sample test and optimizes a lower-bound of test power via an auxiliary generative model. For this method, we used window sizes $w \in [10, 25]$ for all experiments, and trained the model for 25 epochs, unless more training led to improved results. Consistent with our own post-processing steps, we performed peak detection based on the adaptive scale selection method to detect the exact time of change.

In addition to the baseline methods, we also do an ablation study and report the performance of the separate parts of TiVaCPD score, namely the time-varying correlation score (CovScore) and the Dynamic MMD score (DistScore).

Roerich [Hushchyn and Ustyuzhanin, 2021] A direct density ratio estimation based CPD method. We set the *net* and *scalar* parameters to default, and used window sizes $w \in [10, 25]$ for all experiments.

Group Fused Graph Lasso (GraphTime) [Gibberd and Nelson, 2015] GraphTime is a time-varying graphical model based on the group fused-lasso. We used the default parameters provided by the authors.

4.3 Evaluation

Tables 1-3 show performance of TiVaCPD and all baselines on 4 simulated data sets. The results are reported using F_1 score that measures the performance of the methods in detecting the location of CPs in time, as well as precision and recall. We use the previously defined peak-detection algorithm to pinpoint the exact time of change for TiVaCPD as well as all baselines. For estimating performance metrics,

¹For the implementation of the baselines, we have used the publicly released source code by the authors

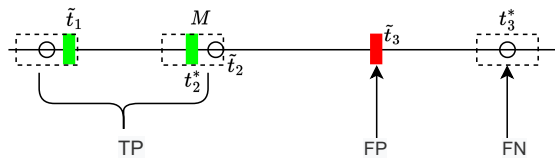


Figure 4: Definition of margin of error. The ground truth CPs t^* are shown as circles and \tilde{t} are the CPs detected by a CPD method. The prediction is a true positive if \tilde{t} falls within the margin around the ground truth.

we define a margin of error M for the exact location of CP, which is a common practice in CPD literature [van den Burg and Williams, 2020, Deldari et al., 2021]. Given a user-defined margin of error, $M > 0$, an estimated CP is a True Positive (TP) if the distance between the ground-truth (t^*) and the estimated CP (\tilde{t}) is smaller than the margin of error, i.e. $|t^* - \tilde{t}| \leq M$. As shown in Figure 4, if an estimated CP falls outside the margin around the closest ground truth CP, then it is deemed a False Positive (FP), i.e. $\tilde{t} \notin [t^* - M/2, t^* + M/2]$. For some of our datasets, we show how different margin values $M = \{5, 10\}$ impact the performance of all models and a more comprehensive set of results for all other datasets are presented in the Appendix.

In each simulated dataset with specific type of CPs, we see that the different parts of the TiVaCPD score captures the particular type of CPs better. In Changing Correlation dataset, only CovScore is able to detect the CP and in other cases like Jumping Mean or Changing Variance, DistScore detects the CPs better. In the Arbitrary CPs dataset where a mixture of CP types are simulated, we can see that the different components of TiVaCPD separately identify various types of CPs. But more importantly, we show that the ensemble score combines the strength of each component and as a result, TiVaCPD score outperforms all other baselines. Note that the performance is not just a result of ensembling the scores, but each component of the score by itself does a better job at detecting the relevant CPs in comparison to baseline methods. Among other baselines, GraphTime is the only method that incorporates different types of CPs into its detection algorithm and therefore often performs second best. The performance results on the real-life datasets are reported in Table 4, for all baselines with a margin value of 10. We show that our method outperforms all baselines in detecting the the exact time of CP in real-world datasets as well as the simulations. Figure 3 shows a graphical representation and comparison of the different CPD methods for a time series sample (row 1), and demonstrates how different methods generate scores for CPs. Different components of TiVaCPD are shown in rows 2 and 3, and show what category of CPs they identify. The heatmaps of CovScore can be used to identify in which pair of features the change in correlation has occurred, and

Method	Jumping Mean			Changing Variance		
	Precision	Recall	F1 (M=5)	Precision	Recall	F1 (M=5)
TiVaCPD	0.80 (0.15)	0.9 (0.10)	0.83 (0.12)	0.56 (0.12)	0.70 (0.16)	0.63 (0.14)
TiVaCPD-CovScore	0.51 (0.17)	0.85 (0.10)	0.60 (0.16)	0.24 (0.10)	0.68 (0.17)	0.34 (0.11)
TiVaCPD-DistScore	1.00 (0.00)	0.67 (0.12)	0.80 (0.09)	0.89 (0.16)	0.55 (0.14)	0.67 (0.15)
KL-CPD	0.20 (0.04)	0.73 (0.16)	0.31 (0.07)	0.12 (0.04)	0.72 (0.17)	0.20 (0.07)
Roerich	0.50 (0.23)	0.35 (0.15)	0.41 (0.18)	0.07 (0.09)	0.08 (0.09)	0.07 (0.09)
GraphTime	0.92 (0.10)	0.70 (0.14)	0.78 (0.10)	0.10 (0.02)	1.00 (0.00)	0.10 (0.02)

Table 1: Performance of CPD methods on the Jumping Mean and Changing Variance datasets using a margin of 5.

Method	Changing Correlations			Arbitrary CPs		
	Precision	Recall	F1 (M=5)	Precision	Recall	F1 (M=5)
TiVaCPD	0.67 (0.08)	1.00 (0.00)	0.80 (0.06)	0.71 (0.05)	1.00 (0.00)	0.83 (0.03)
TiVaCPD-CovScore	0.48 (0.07)	1.00 (0.00)	0.64 (0.06)	0.39 (0.14)	1.00 (0.00)	0.54 (0.16)
TiVaCPD-DistScore	0.00 (0.00)	0.00 (0.00)	0.00 (0.00)	0.98 (0.05)	0.65 (0.15)	0.76 (0.11)
KL-CPD	0.14 (0.05)	0.70 (0.22)	0.23 (0.08)	0.19 (0.06)	0.85 (0.15)	0.31 (0.01)
Roerich	0.15 (0.10)	0.15 (0.10)	0.15 (0.10)	0.50 (0.16)	0.35 (0.10)	0.41 (0.11)
GraphTime	0.21 (0.04)	0.98 (0.06)	0.35 (0.06)	0.35 (0.11)	0.78 (0.13)	0.46 (0.10)

Table 2: Performance of CPD methods on the Changing Correlations and Arbitrary CPs datasets using a margin of 5.

Method	Changing Correlations			Arbitrary CPs		
	Precision	Recall	F1 (M=10)	Precision	Recall	F1 (M=10)
TiVaCPD	0.67 (0.08)	1.00 (0.00)	0.80 (0.06)	0.71 (0.05)	1.00 (0.00)	0.83 (0.03)
TiVaCPD-CovScore	0.53 (0.10)	1.00 (0.00)	0.69 (0.08)	0.41 (0.16)	1.00 (0.00)	0.54 (0.18)
TiVaCPD-DistScore	0.00 (0.00)	0.00 (0.00)	0.00 (0.00)	0.90 (0.04)	0.65 (0.15)	0.76 (0.11)
KL-CPD	0.20 (0.09)	0.85 (0.09)	0.21 (0.11)	0.20 (0.06)	0.98 (0.06)	0.33 (0.09)
Roerich	0.37 (0.18)	0.33 (0.09)	0.33 (0.11)	0.48 (0.19)	0.35 (0.13)	0.40 (0.14)
GraphTime	0.18 (0.04)	1.00 (0.00)	0.30 (0.05)	0.35 (0.13)	0.8 (0.11)	0.45 (0.13)

Table 3: Performance of CPD methods on the Changing Correlations and Arbitrary CPs datasets using a margin of 10.

Method	Bee Dance			HAR		
	Precision	Recall	F1	Precision	Recall	F1
TiVaCPD	0.63 (0.20)	0.56 (0.24)	0.59 (0.22)	0.76 (0.16)	0.75 (0.20)	0.71 (0.13)
TiVaCPD-CovScore	0.63 (0.20)	0.56 (0.24)	0.59 (0.22)	0.76 (0.16)	0.75 (0.20)	0.71 (0.06)
TiVaCPD-DistScore	0.52 (0.22)	0.35 (0.26)	0.41 (0.25)	0.74 (0.12)	0.33 (0.10)	0.45 (0.09)
KL-CPD	0.28 (0.15)	0.81 (0.22)	0.39 (0.15)	0.35 (0.09)	0.60 (0.15)	0.43 (0.10)
Roerich	0.46 (0.37)	0.17 (0.09)	0.25 (0.14)	0.61 (0.21)	0.14 (0.05)	0.23 (0.08)
GraphTime	0.13 (0.04)	0.85 (0.16)	0.22 (0.06)	0.04 (0.01)	0.92 (0.05)	0.07 (0.01)

Table 4: Performance of multiple CPD methods on the Bee Dance dataset.

also in which direction was the change in correlation.

5 Conclusion

In this paper, we introduce TiVaCPD, a novel CP detection method that characterizes the different types of CPs in time series. Each component of our score identifies a different type of CP, that is either caused by a change in distribution

or a change in the dynamics of the time series features. We identify the changes in feature dynamics and are able to characterize the CP based on the change in correlation networks. Investigating the different components of our score can help with better understanding of the causes of the detected change points.

References

- Julien Ah-Pine. Normalized kernels as similarity indices. In *Pacific-Asia Conference on Knowledge Discovery and Data Mining*, pages 362–373. Springer, 2010.
- Samaneh Aminikhanghahi and Diane J. Cook. A survey of methods for time series change point detection. *Knowledge and Information Systems*, 51:339–367, 2017.
- Davide Anguita, Alessandro Ghio, Luca Oneto, Xavier Parra, and Jorge L. Reyes-Ortiz. A public domain dataset for human activity recognition using smartphones. In *European Symposium on Artificial Neural Networks, Computational Intelligence and Machine Learning*, 2013.
- Michèle Basseville and Igor Nikiforov. Detection of abrupt change theory and application. 1993.
- Wei-Cheng Chang, Chun-Liang Li, Yiming Yang, and Barnabás Póczos. Kernel change-point detection with auxiliary deep generative models. In *International Conference on Learning Representations*, 2019.
- Kevin C Cheng, Shuchin Aeron, Michael C Hughes, Erika Hussey, and Eric L Miller. Optimal transport based change point detection and time series segment clustering. In *ICASSP 2020-2020 IEEE International Conference on Acoustics, Speech and Signal Processing*, pages 6034–6038. IEEE, 2020.
- Shohreh Deldari, Daniel V. Smith, Hao Xue, and Flora D. Salim. Time series change point detection with self-supervised contrastive predictive coding. *WWW '21: Proceedings of the Web Conference*, 2021.
- Alexander J. Gibberd and James D.B. Nelson. Estimating dynamic graphical models from multivariate time-series data. In *International Workshop on Advanced Analytics and Learning on Temporal Data*, 2015.
- Arthur Gretton, Karsten M Borgwardt, Malte Rasch, Bernhard Schölkopf, and Alex J Smola. A kernel method for the two-sample-problem. *International Conference on Neural Information Processing*, 2007.
- Arthur Gretton, Dino Sejdinovic, Heiko Strathmann, Sivaraman Balakrishnan, Massimiliano Pontil, Kenji Fukumizu, and Bharath K. Sriperumbudur. Optimal kernel choice for large-scale two-sample tests. *International Conference on Neural Information Processing*, 2012.
- Fredrik Gustafsson. The marginalized likelihood ratio test for detecting abrupt changes. *IEEE Transactions on automatic control*, 1996.
- David Hallac, Youngsuk Park, Stephen Boyd, and Jure Leskovec. Network inference via the time-varying graphical lasso. In *23rd ACM SIGKDD International Conference on Knowledge Discovery and Data Mining*, pages 205–213, 2017.
- Mikhail Hushchyn and Andrey Ustyuzhanin. Generalization of change-point detection in time series data based on direct density ratio estimation. *Journal of Computational Science*, 53:101385, 2021.
- Yoshinobu Kawahara, Takehisa Yairi, and Kazuo Machida. Change-point detection in time-series data based on subspace identification. *The IEEE International Conference on Data Mining (ICDM)*, 2007.
- Marc Lavielle and Gilles Teyssière. Adaptive detection of multiple change-points in asset price volatility. *Long Memory in Economics*, 2007.
- Shuang Li, Yao Xie, Hanjun Dai, and Le Song. M-statistic for kernel change-point detection. *International Conference on Neural Information Processing*, 2015.
- David S. Matteson and Nicholas A. James. A nonparametric approach for multiple change point analysis of multivariate data. *Journal of the American Statistical Association*, 109, 2014.
- Sang Min Oh, James M. Rehg, Tucker Balch, and Frank Dellaert. Learning and inferring motion patterns using parametric segmental switching linear dynamic systems. In *International Journal of Computer Vision (IJCV) Special Issue on Learning for Vision*, pages 103–124, 2008.
- William H. Press and Saul A. Teukolsky. Savitzky-golay smoothing filters. *Computers in Physics 4, Volume 4*, 1990.
- Jaxk Reeves, Jien Chen, Xiaolan L. Wang, Robert Lund, and Qi Qi Lu. A review and comparison of changepoint detection techniques for climate data. *Journal of Applied Meteorology and Climatology*, 46, 2007.
- Felix Scholkmann, Jens Boss, and Martin Wolf. An efficient algorithm for automatic peak detection in noisy periodic and quasi-periodic signals. *Algorithms*, 2012.
- Antonin Schrab, Ilmun Kim, Mélisande Albert, Béatrice Laurent, Benjamin Guedj, and Arthur Gretton. Mmd aggregated two-sample test, 2021. URL <https://arxiv.org/abs/2110.15073>.
- Charles Truong, Laurent Oudre, and Nicolas Vayatis. Selective review of offline change point detection methods. *Signal Processing Volume 167*, 2018.
- Gerrit J. J. van den Burg and Christopher K. I. Williams. An evaluation of change point detection algorithms. *arXiv:2003.06222v2 [stat.ML]*, 2020.
- Kenji Yamanishi and Jun-ichi Takeuchi. A unifying framework for detecting outliers and change points from non-stationary time series data. *Proceedings of the eighth ACM SIGKDD international conference on Knowledge discovery and data*, pages 676–681, 2002.
- Ping Yang, Dumont Guy, and J Mark Ansermino. Adaptive change detection in heart rate trend monitoring in anesthetized children. *IEEE Transactions on Biomedical Engineering*, 2007.